

FINE STRUCTURE OF BANDS IN VIBRATIONAL SPECTRA OF C₆₀ FULLERITE

M.E. KORNIENKO, M.P. KULISH, S.A. ALEKSEEV, O.P. DMYTRENKO, O.L. PAVLENKO

PACS 78.30.Na, 78.40.Ri
©2010

Taras Shevchenko National University of Kyiv
(64, Volodymyrs'ka Str., Kyiv 01601)

We investigated the fine structure of low-frequency vibrational bands in the Raman, infrared absorption, and diffuse reflectance spectra of C₆₀ fullerite. It is related to the components of the overlapping Davydov and isotope splittings, as well as to a possible splitting of vibrations due to a reduction of the symmetry. It is shown that the splittings for the Raman $H_g(1)$ and $A_g(1)$ bands and the IR $F_u(1,2)$ bands at room temperature are larger than those in the low-temperature phase. The intensification of the intermolecular interaction at higher temperatures is explained by the nonequilibrium vibrational excitation of the medium due to the nonlinear interaction of vibrational modes and a change of energy states.

1. Introduction

Investigations of various forms of fullerites are of large interest for the solution of both fundamental and applied problems. An important role is played by the high symmetry of C₆₀ molecules and the resulting considerable degeneracy of their electron and vibrational states. The degeneracy provides a high sensitivity of vibrational spectra of fullerenes to the influence of comparatively weak perturbations that result in a reduction of the symmetry and the violation of the degeneracy. The reduction of a symmetry of the medium is possible due to the influence of intermolecular interactions and the crystal field, as well as due to the presence of isotopes and polymerization [1, 2]. In the case of the icosahedral symmetry I_h , the symmetry reduction can result in the splitting of the fivefold degenerate H_g vibrations of C₆₀ fullerenes into the $E_g + F_g$ vibrations [1, 3] or even into singly degenerate vibrations, which gives rise to the appearance of a maximal number of components of the fine structure of vibrational bands. For example, the splitting of the H_g mode into the nondegenerate vibrations $2A_g + B_g(1) + B_g(2) + B_g(3)$ allowed in Raman spectra are realized under the symmetry reduction for C₆₀ fullerites to D_{2h} for their orthorhombic structure [4]. For this symmetry, the triply degenerate F_u dipole modes active in IR-absorption also split into the simple vibra-

tions $B_g(1) + B_g(2) + B_g(3)$. The symmetry reduction also can result in the appearance of “silent” vibrations in vibrational spectra, for example, of the G_g type [1], which increases the informativity of spectral methods.

In IR absorption spectra of C₆₀ fullerenes, there are four allowed modes $F_u(j)$, ($j = 1-4$). While in Raman spectra, there are ten vibrations (two totally symmetric nondegenerate modes $A_g(1)$, $A_g(2)$ and eight modes $H_g(i)$, ($i = 1-8$)). The fine structure of vibrational bands in the Raman and IR reflectance spectra of C₆₀ fullerite was studied in [1,5,6]. The use of pure ¹²C₆₀ and ¹³C₆₀ isotopes allowed one to separate crystal and isotope splittings. At the temperature $T=10$ K, the $F_u(1)$ band included four Davydov components, the $F_u(3,4)$ bands – three of them, whereas the $F_u(2)$ band remained one-component [5]. In the Raman spectrum, the fine structure of individual vibrational bands of C₆₀ fullerite was studied between the helium temperature (2 K) and the phase-transition temperature of C₆₀ fullerite close to 260 K [1], at which a simple cubic lattice is turned into a high-temperature face-centered cubic (FCC) structure. The $H_g(1)$ and $H_g(4)$ bands of isotope-free fullerenes contained 4 components arisen due to the crystal splitting, while the strong $A_g(2)$ band – two components [1]. Thus, both the threefold degenerate $F_u(1)$ mode and the fivefold degenerate $H_g(1)$ and $H_g(4)$ ones are split into four spectral components, which coincides with the number of molecules in a unit cell of C₆₀ fullerite both in a simple cubic structure and in a face-centered cubic one [3]. That is why the discussed splittings must be considered as Davydov ones. In fullerites with the natural isotope content, one observes a larger number of fine-structure components due to the isotope splitting. At room temperature, all bands are widened, and their structure becomes diffused.

It was considered till now that, in the high-temperature phase of fullerite ($T > 260$ K), the orientation disordering of C₆₀ molecules results in a considerable weakening of the crystal-field effects and a possible Davydov splitting. At the same time, according to [1],

the positions of the components in the Davydov multiplet for the most low-frequency Raman band $H_g(1)$ change very little as the temperature increases from 2 K to 261 K. It is also worth noting that the fine structure of vibrational bands at high temperatures was observed for polymerized samples [4], while the structure of the $A_g(2)$ band observed in [7] was related to the Fermi resonance due to the interaction with the $3A_g(1)$ overtone, rather than to the crystal splitting. Thus, the mechanisms of formation of the fine structure of vibrational bands of C_{60} fullerenes are investigated incompletely. In addition, it should be taken into account that, with increase in the temperature, the registration of a fine structure is complicated by the strong overlapping of individual components. That is why one must use special techniques, for example second-derivative spectra and the forbidden bands of isolated molecules often observed as a result of the intermolecular interaction [8–11].

In the given work, we study the fine structure of the most low-frequency bands $H_g(1)$, $A_g(2)$ in Raman spectra and IR absorption $F_u(1,2)$, a part of which manifested the strongest Davydov splitting. In order to increase the reliability of our results, we used both IR transmission and diffuse reflectance spectra. The splittings of the $F_u(1,2)$ bands obtained by two spectral techniques are compared. Considerable Davydov splittings in the high-temperature phase of C_{60} fullerite are related to the intensification of the intermolecular interaction due to a nonequilibrium vibrational excitation of the medium.

2. Experimental Technique and Materials

We investigated C_{60} fullerite films with the thicknesses $d = 1.2$ and $2 \mu\text{m}$ on a Si(100) silicon substrate. The IR absorption and reflectance spectra were studied with the help of a Nicolet NEXUS-470 Fourier spectrometer. Oscillations in the IR transmission spectra resulting from the interference in a plane-parallel silicon plate were removed by means of the numerical smoothing. The Fresnel losses at the input and output surfaces of the samples were taken into account. For this purpose, we determined the attenuation of radiation due to reflection and scattering at the edges of the sample using the transmission spectrum $T(\nu)$ in the regions of maximal transparency and allowed for it by introducing the corresponding background level $T_F(\nu)$. After that, we calculated the optical density spectra $D(\nu) = -\ln [T(\nu)/T_F(\nu)]$. The Raman spectra were excited by radiation of a continuous Ar^+ laser ($\lambda_L = 514.5 \text{ nm}$). They were registered with the help of an automa-

tized double DFS-24 monochromator with a cooled photomultiplier and a registration system operating in the photon-counting mode. In order to decrease the photopolymerization of C_{60} , we used the cylindrical focusing of laser radiation (the spot size was $0.3 \times 2.5 \text{ mm}^2$), whose intensity approximated 2 W/cm^2 . The signal/noise ratio was increased by means of the signal accumulation (in particular, we used 128 scanings in the IR spectrometer), as well as the optimal numerical smoothing of spectra with the fitting of the number of smoothing points. All experimental investigations were carried out at room temperature (295 K).

Vibrational bands were extracted numerically at the wide-band background of vibrational spectra by means of their polynomial approximation with the use of a necessary number of experimental points. The frequency positions of individual spectral components, their intensities, shapes, and half-widths were determined with the help of the numerical decomposition of vibrational bands into elementary spectral components. The number of reliable components for each band was determined by the number of negative minima of the second derivatives $y^{(2)}$ calculated according to experimental data. In order to decrease noises in $y^{(2)}$, we carried out their optimal smoothing. The consistency of the numerical decomposition of the bands into individual components was controlled by matching the second derivatives of the experimental and calculated contours of vibrational bands.

3. Results and Their Discussion

3.1. General analysis of Raman and IR absorption and reflectance spectra of C_{60} fullerite films

The most intense Raman bands of the totally symmetric vibrations $A_g(1)$ and $A_g(2)$ of C_{60} molecule corresponding to the radial breathing mode and shifts of C atoms along the edges of a truncated icosahedron [7], as well as the rather intense low-frequency $H_g(1)$ band for the $2\text{-}\mu\text{m}$ fullerite sample, are shown in Fig. 1, *a*. These bands with maximum frequencies of 271, 497, and 1470 cm^{-1} are characterized by a low-frequency asymmetry and the presence of high-frequency shoulders at 297, 501, and 1482 cm^{-1} , which must be explained by general physical reasons. To a large degree, the asymmetric structure of the considered bands of C_{60} fullerite is caused by the common influence of the Davydov splitting and the resonance generation of difference and summation tones, as well as by a possible contribution of vibrations of C_{60} molecules in the excited triplet state [12]. For example,

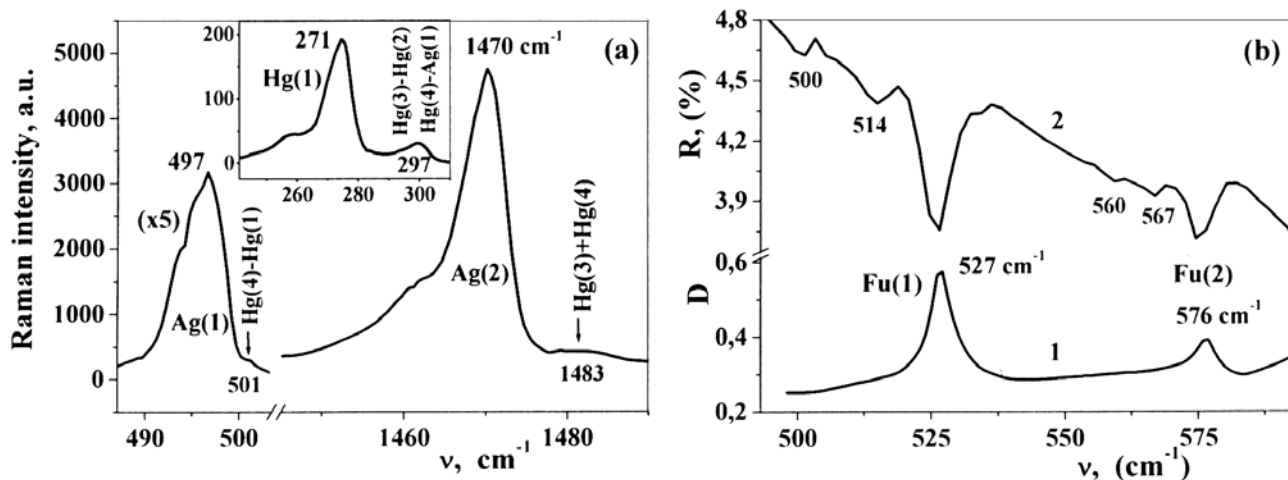


Fig. 1. Vibrational bands $H_g(1)$, $A_g(1)$, and $A_g(2)$ in the Raman spectrum ($\lambda_L = 514.5$ nm, $T = 295$ K) (a) and fragments of optical density (1) and diffuse reflectance (2) spectra (b) of the 2- μm (a) and 1.2- μm (b) C_{60} fullerite films

the difference frequency $H_g(4) - H_g(1)$ ($773 - 271 = 502$ cm^{-1}) corresponds to the high-frequency shoulder of the $A_g(1)$ band. The pronounced high-frequency maximum at 297 cm^{-1} close to the $H_g(1)$ band is related to the difference tones $H_g(3) - H_g(2)$ and $H_g(4) - A_g(1)$. The high-frequency shoulder of the strong $A_g(2)$ band correlates with the summation tone $H_g(3) + H_g(4)$ with a calculated frequency of 1482 cm^{-1} .

The obtained IR spectra of the optical density $D(\nu)$ that contain the fundamental $F_u(1,2)$ bands of C_{60} fullerite and the diffuse reflectance spectra are presented in Fig.1,b. Same as the bands of totally symmetric vibrations in the Raman spectrum, these IR bands are rather sharp. The most intense band in the IR spectrum is the $F_u(1)$ band with a maximum frequency of 527 cm^{-1} , whose highest value of the absorption coefficient $\alpha(\nu) = D(\nu)/d$ (d is the sample thickness) exceeds 2500 cm^{-1} . The diffuse reflectance spectrum of the 1.2- μm fullerite film was studied with the use of a Spectra-Tech Inc. cell (model 0001-397). A contribution into this spectrum is made by the whole thickness of the fullerite film, as one observes two orders of the thin-film interference in it. At the same time, the near-surface region of the film gives a greater contribution as compared with that to the absorption spectrum. As is known, the reflectance spectra are formed with participation of the real and imaginary parts of the complex refractive index. At the same time, in contrast to common mirror reflection spectra [5], the diffuse reflection is characterized by the attenuation of IR radiation in the region of absorption bands. That is why these spectra

approach the transmission ones, which simplifies obtaining the spectral information.

The investigated IR bands (like the Raman ones) are characterized by a low-frequency asymmetry, whereas the reflectance spectra have a pronounced fine structure that contains additional components at 500 , 514 cm^{-1} and 560 , 567 cm^{-1} (Fig. 1,b). It is worth noting that, at room temperature, we did not register the crystal splitting of IR bands in the reflectance spectra of C_{60} fullerite [5]. It is explained by a large total width of general reflection bands that reveal both absorption bands and a dispersion of refractive indices in wider regions near the fundamental absorption bands. The component close to 500 cm^{-1} (like the high-frequency shoulder of the $A_g(1)$ Raman band) can be attributed to the difference tone $H_g(4) - H_g(1)$. In the region 500 – 590 cm^{-1} , one can also register the second-order bands $2H_g(1)$ and $H_g(6) - H_g(3)$ with the calculated frequencies equal to 540 and 544 cm^{-1} . That is why the majority of the present components in the region of the $F_u(1,2)$ bands should be related to the Davydov splitting. This fact is also confirmed by the results of studying the structure of these absorption bands.

3.2. Davydov splitting of $H_g(1)$, $A_g(1)$, and $F_u(1,2)$ vibrational bands

It is important that the $H_g(1)$ and $A_g(1)$ vibrations in the Raman spectrum are characterized by different degeneracies. The $A_g(1)$ mode is nondegenerate, while the $H_g(1)$ one is fivefold degenerate. Comparing the splittings for these vibrations, one can separate the contribu-

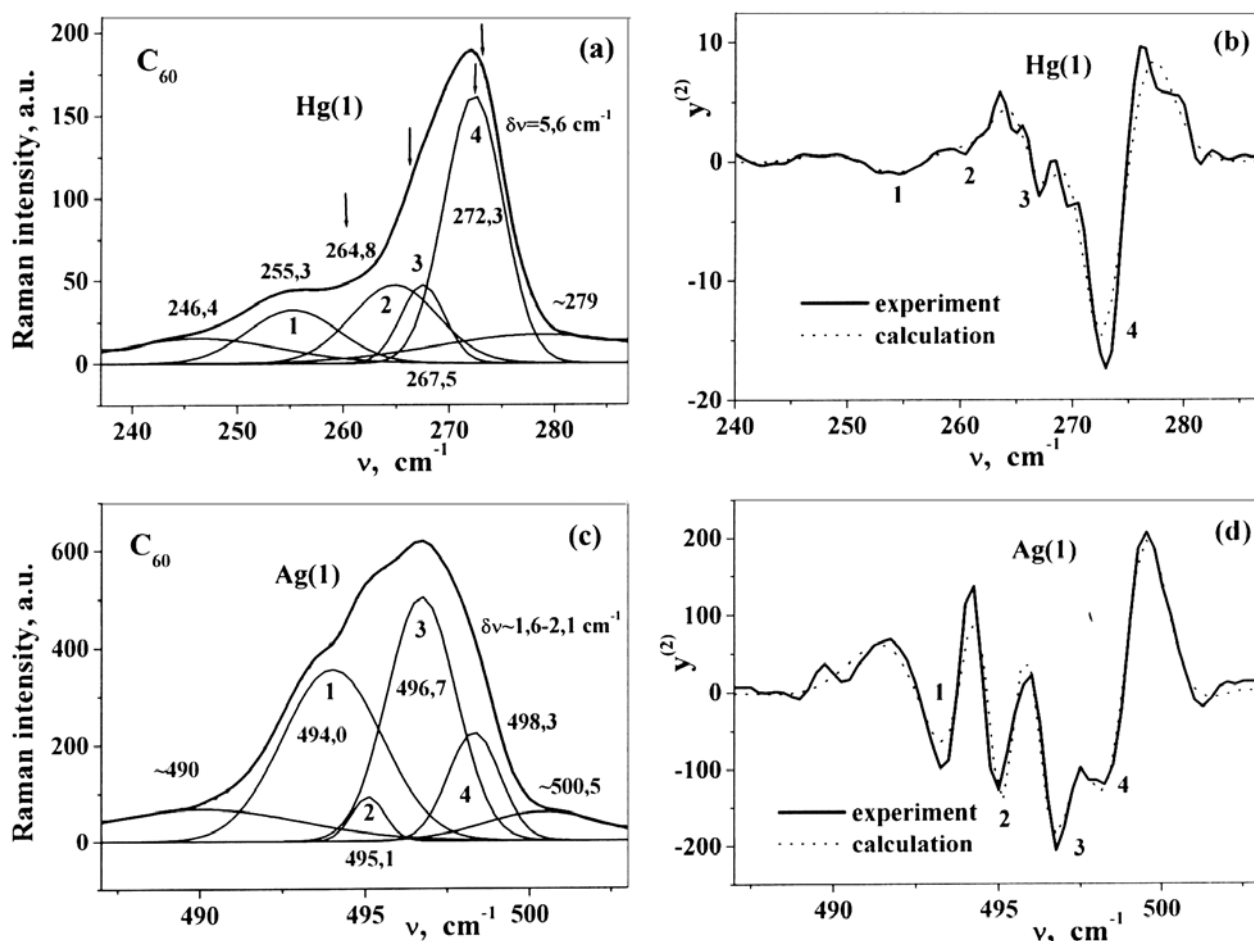


Fig. 2. Decomposition of the vibrational bands $H_g(1)$ (a) and $A_g(1)$ (c) in the Raman spectrum ($T=295$ K; 514.5 nm) of the $2\text{-}\mu\text{m}$ C_{60} fullerite film into Gaussian spectral components and the comparison of the second derivatives of the experimental and calculated forms of the $H_g(1)$ (b) and $A_g(1)$ (d) bands

tions of collective effects of the crystal field and a possible isotope splitting [1, 5]. For the $H_g(1)$ band, one observes two spectral components at 266.3 and 272.3 cm^{-1} for $T = 261$ K, while there appear two more additional components at 260 and 273 cm^{-1} below 259 K. The results of numerical decomposition of the $H_g(1)$ and $A_g(1)$ bands into individual spectral components are illustrated in Fig. 2. It turns out that these bands can be well described by a sum of Gaussian spectral components. In the decomposition of the central part of the $H_g(1)$ band, one observes at least 4 components lying at 255 , 265 , 267.5 , and 272.3 cm^{-1} that correspond to the minima in the second-derivative spectrum calculated according to the experimental data (Fig. 2,b). The main components of the fine structure of the Raman $H_g(1)$ band in Figs. 2,a and 2,b are marked by figures 1–4. A

good agreement between the second derivatives of the experimental and calculated contours of the $H_g(1)$ band testifies to the consistency of the performed numerical decomposition.

The arrows in Fig. 2,a mark the positions of the sharp components of the crystal splitting in the Raman spectra of the low-temperature phase of C_{60} fullerite [1]. One can see that the main components of the fine structure of the $H_g(1)$ band in the region of room temperatures are mainly in good agreement with the known components of the Davydov splitting in the temperature range $2\text{--}259$ K. It is worth noting that, for the high-temperature FCC phase of C_{60} fullerite, one also observes a low-frequency asymmetry of the fine structure of the given band like that at low temperatures [1]. Due to this fact, this splitting can be rated as the Davydov one.

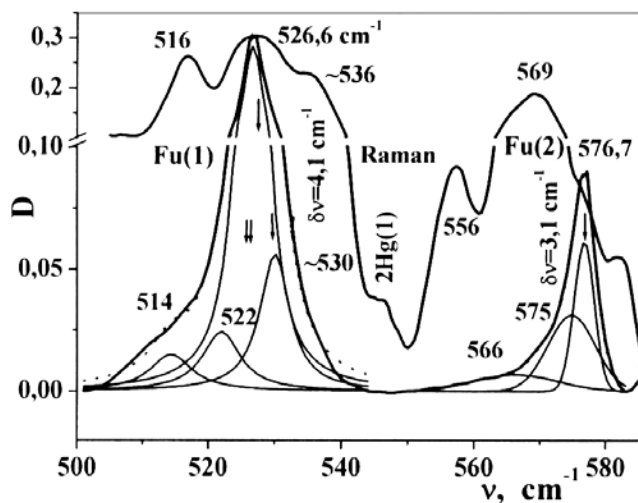


Fig. 3. Decomposition of the $F_u(1)$ and $F_u(2)$ bands into Lorentz and Gaussian components, respectively, and their comparison with the observed forbidden Raman bands ($T = 295$ K; 514.5 nm) normalized to the maximum of the $F_u(1)$ IR band

Such an interpretation agrees with the splitting for the nondegenerate $A_g(1)$ mode, which is illustrated in Fig. 2, *c*. A decomposition into spectral components and a good agreement of the second derivatives for the experimental and calculated forms of the contours in the case of the Raman $A_g(1)$ band can be also obtained allowing for four central components close to 494 , 495 , 497 , and 498 cm^{-1} , which is shown in Fig. 2, *c*. One can demonstrate that the wider side components with the maxima close to 490 and 501 cm^{-1} are related to different components of the difference tone $H_g(4) - H_g(1)$. The comparison between the second derivatives $y^{(2)}$ of the experimental and calculated $A_g(1)$ bands is presented in Fig. 1, *d*. One can see that the Davydov components correspond to the pronounced minima of $y^{(2)}$. Due to the presence of the ^{13}C isotope (1.11%), there can appear another low-frequency component for the nondegenerate $A_g(1)$ vibration that corresponds to the minimum of $y^{(2)}$ close to 490 cm^{-1} . The additional isotope splitting can also result in a large half-width of low-frequency component 1 in Fig. 2, *c*. Thus, the registration of four spectral components for the nondegenerate $A_g(1)$ mode testifies to the existence of the Davydov splitting caused by the presence of four molecules in the unit cell of C_{60} fullerite [3].

According to Fig. 2, *c*, the total splitting of the $A_g(1)$ band exceeds 4 cm^{-1} in spite of the fact that we did not observe any splitting for this band at lower temperatures, which can be due to its small magnitude.

The splitting for the $H_g(1)$ band in the region of the high-temperature FCC phase of C_{60} fullerite increases to 17 cm^{-1} , which exceeds the total splitting equal to 13 cm^{-1} at 2 K. It is worth noting that, in the region of low-frequency component 1 of the considered $H_g(1)$ splitting, the complex form of the second derivative in Fig. 2, *b* can be related to the contribution of the difference tone $F_u(1) - H_g(1)$. The basic difference of the splittings of vibrational bands in the high-temperature FCC phase consists in a considerable widening of individual spectral components, though the total magnitude of splitting can even grow. The increase of the splitting related to the migration of excitation in a crystal testifies to the intensification of the intermolecular interaction due to the stronger thermal excitation of fullerite.

Due to the symmetry reduction of the medium, we additionally observed the bands of the IR-active vibrations $F_u(1)$ and $F_u(2)$ with the maxima at 527 and 569 cm^{-1} in the Raman spectrum. The comparison of these Raman bands normalized to the maximum of the $F_u(1)$ one with the IR bands $F_u(1,2)$ is given in Fig. 3. We note the much larger width of the Raman-forbidden bands, which is typical of this kind of bands [13]. We also present there the decomposition of the IR-allowed $F_u(1,2)$ bands into individual spectral components. For the sake of comparison, the arrows in Fig. 3 mark the positions of the components of the Davydov splitting of the $F_u(1)$ band for a temperature of 10 K, as well as the position of the $F_u(2)$ band in the case of the low-temperature phase [5].

It is worth noting that the structures of the $F_u(1,2)$ bands in the scattering and absorption spectra are close and agree with the diffuse reflectance spectrum (Fig. 1, *b*). For example, in the absorption and diffuse reflectance spectra for the $F_u(1)$ band, one observes a low-frequency component at 514 cm^{-1} corresponding to the Raman component at 516 cm^{-1} . The high-frequency shoulder close to 546 cm^{-1} can be related to the $2H_g(1)$ overtone. The weak 560 - cm^{-1} and 567 - cm^{-1} components in the $F_u(2)$ reflectance band (see Fig. 1, *b*) are close to the fundamental maxima at 556 and 569 cm^{-1} in the Raman band. Good agreement of the fundamental spectral components for the $F_u(1,2)$ bands in the Raman and IR spectra confirms the reliability of the structure of the fullerite vibrational bands observed at room temperature.

The splitting of the $F_u(1,2)$ IR bands can be related to the symmetry reduction of molecules due to the intermolecular interaction. However, the presence of four spectral components in the decomposition of the band for the triply degenerate $F_u(1)$ mode in Fig. 3, which coincides both with the results obtained at low temper-

atures [5] and with the number of the splitting components for the nondegenerate $A_g(1)$ band, confirms the presence of the Davydov splitting. According to the data given in Fig. 3, the total magnitude of the Davydov splitting $\Delta\nu$ for the $F_u(1)$ and $F_u(2)$ bands amounts to $\sim 16 \text{ cm}^{-1}$ and $\sim 10 \text{ cm}^{-1}$, respectively. In the case of the isotope-free $^{12}\text{C}_{60}$ sample, the Davydov splitting of the $F_u(1)$ band at a temperature of 10 K is equal to 3.25 cm^{-1} . Thus, the Davydov splittings in the $F_u(1,2)$ IR bands in the high-temperature phase of C_{60} fullerite are larger than those in the low-temperature region.

3.3. Intensification of intermolecular interaction due to vibrational excitation of the medium

The largest splittings ($\Delta\nu=16\text{-}17 \text{ cm}^{-1}$) are observed for the most low-frequency bands $H_g(1)$ and $F_u(1)$, which is possibly caused by their considerable thermal excitation. An increase in the splitting of all bands at room temperature as compared with that at low temperatures testifies to the intensification of the intermolecular interaction and an acceleration of the spatial energy migration in the high-temperature phase of C_{60} fullerite. The magnitudes of $\Delta\nu$ lie between their values characteristic of the low-temperature and polymerized phases of fullerenes. For example, according to Fig. 2, *a*, the extreme splitting components for the $H_g(1)$ band lie at 255 and 272 cm^{-1} , whereas they are close to 249 and 276 cm^{-1} [4] for a polymerized sample, i.e., the splitting widens to the both sides. The obtained results allow one to assume that the polymerization mechanism of fullerenes is related to the magnitudes of the Davydov splitting, i.e. to collective mechanisms of migration of the excitation energy in the C_{60} crystal.

The difference in the positions of the maxima of the $F_u(2)$ bands in the Raman and IR spectra (7 cm^{-1}) also testifies to the existence of rather strong intermolecular interactions in the high-temperature phase of fullerite. It is caused by the differences in the wave vectors k of vibrational states that manifest themselves in various techniques of vibrational spectroscopy and can characterize the lower limit for the width of the existing phonon band. Taking into account that vibrational states observed in Raman spectra are characterized by large k , the lower 569-cm^{-1} frequency can testify to the negative dispersion $\nu(k)$ of the fullerite phonon band related to the $F_u(2)$ mode. The maximal widths of phonon bands should be expected for dipole vibrations due to the intensification of their intermolecular interaction.

The complex structure of the Raman bands for the FCC phase of C_{60} fullerenes indicates the presence of special mechanisms of intensification of the intermolecular interaction in the high-temperature region. At room temperature $\sim 295 \text{ K}$, a considerable thermal excitation of low-frequency modes makes one assuming the existence of a substantial intensification of their nonlinear interaction with the generation of a nonequilibrium population of high vibrational states. The efficiency of this mode interaction considerably increases due to the resonance nature of these processes, particularly due to the existence of a number of resonances: $H_g(1) + H_g(2) = H_g(3)$; $H_g(1) + A_g(1) = H_g(4)$; $H_g(3) + H_g(4) = A_g(2)$, etc. Another characteristic feature of such wave nonlinear processes is their spatial accumulation [10,13–16]. The registration of additional components close to 297 and 501 cm^{-1} for the Raman $H_g(1)$ and $A_g(1)$ bands testifies to the reality of the nonlinear interaction of vibrational modes of fullerenes and a possibility of due to generation of the summary frequencies $H_g(1) + H_g(2)$ and $H_g(1) + A_g(1)$ which are resonant with the $H_g(3)$ and $H_g(4)$ modes. Due to the higher-frequency resonance $H_g(3) + H_g(4) = A_g(2)$, the excitation of medium-frequency modes $H_g(3,4)$ can transform to the region of excitation with still larger energies. High vibrational states approach electron states, interact with them, and induce their changes. The intensification of the Davydov splitting for near-surface regions of fullerite observed in diffuse reflectance spectra also confirms the nonlinear nature of the discussed phenomena, as vibrations of surface atoms are characterized by an increased anharmonicity.

Due to the phenomenon of the strong electron-vibrational interaction [17], the intermolecular interactions in C_{60} fullerite for room and higher temperatures take on intermediate values between the van der Waals forces and chemical bonds in polymerized samples.

4. Conclusions

Investigations of the fine structure of low-frequency vibrational bands of the high-temperature FCC phase of C_{60} fullerite performed with the use of the techniques of IR absorption, diffuse reflectance, and Raman scattering spectroscopy have demonstrated that the central parts of the $H_g(1)$ and $A_g(1)$ bands in the Raman spectrum of fullerite obtained at room temperature consist of four spectral components. The $F_u(1)$ IR band in the absorption and diffuse scattering spectra also includes four components. The reliability of the splittings observed for the $F_u(1,2)$ IR bands is confirmed by the similar splittings of these bands in the Raman spectra due to the

intermolecular interaction and the symmetry reduction for C_{60} molecules. For the $H_g(1)$ and $F_u(1)$ vibrational bands, the splittings at room temperature correlate with the crystal splitting in the low-temperature region [1,5]. This fact together with the existence of a similar splitting for the $A_g(1)$ nondegenerate mode testifies to the presence of the Davydov splitting in the FCC phase of fullerite overlapping with the isotope splitting.

We have established an increase of the crystal splitting for the $H_g(1)$ band from 13 cm^{-1} at 2 K to 17 cm^{-1} at 295 K, as well as a considerable increase of the splittings of the $F_u(1,2)$ dipole modes (from 3.25 cm^{-1} at 10 K [5] to $\sim 16\text{ cm}^{-1}$ for $F_u(1)$ in the high-temperature phase), which testifies to the intensification of the intermolecular interaction in the high-temperature FCC phase of fullerite as compared with that in the low-temperature phase, as well as to the strengthening of collective properties of the vibrational modes of C_{60} fullerite. An increase of the Davydov splitting is due to the appearance of a nonequilibrium vibrational excitation of the medium and the considerable electron-vibrational interaction. The vibrational excitation of fullerite is caused by the nonlinear resonance interaction of thermally excited vibrational modes. It is favored by the multiple Fermi–Davydov resonances for vibrational modes and the spatial accumulation of nonlinear wave interactions. The proposed nonlinear conception is confirmed by the registration of the bands of resonance summary and difference frequencies, as well as by an increase of the splitting for the surface regions of fullerite characterized by a larger anharmonicity of vibrations.

1. P.J. Horoyski, M.L. Thewalt, and T.R. Anthony, *Phys. Rev. Lett.* **74**, 194 (1995).
2. Ricco, T. Shiroka, M. Belli, D. Pontiroli, and M. Pagliari, *Phys. Rev. B* **72**, 155437 (2005).
3. T.L. Makarova, *Fiz. Tekhn. Polupr.* **35**, 257 (2001).
4. J. Winter, H. Kuzmany, P.-A. Person, P. Jacobson, and B. Sundquist, *Phys. Rev. B* **54**, 17486 (1996).
5. C.C. Homes, P.J. Horoyski, M.L.W. Thewalt, B.H. Clayman, and T.R. Anthony, *Phys. Rev. B* **52**, 16892 (1995).
6. O.P. Dmytrenko, M.P. Kulish, M.M. Bilyi, V.O. Gubanov, T.I. Rodionova, Ya.I. Vertsimakha, L.A. Matveeva, Yu.I. Prylutskiy, P. Scharff, and T. Braun, *Mol. Cryst. Liq. Cryst.* **385**, [163]/43–[169]/49 (2002).

7. O.N. Bubel', S.A. Vyrko, E.F. Kislyakov, and N.A. Poklonskii, *Pis'ma Zh. Eksp. Teor. Fiz.* **71**, 741 (2000).
8. N.E. Kornienko, *Ukr. Fiz. Zh.* **46**, 546 (2001).
9. M.P. Kulish, O.P. Dmytrenko, Yu.I. Prylutskiy, E.M. Shpilevskiy, M.M. Bilyi, V.A. Gubanov, M. Hietschold, S. Schulze, J. Ulanski, R. Wojciechowski, M. Kozanecki, and P. Scharff, *Thin Sol. Films* **459**, 254 (2004).
10. N.E. Kornienko, *Ukr. Fiz. Zh.* **47**, 361 (2002).
11. M.E. Kornienko and O.V. Krut', *Visn. Kyiv Univ. Ser. Fiz. Mat. Nauky* **1**, 345 (2005).
12. G. Chambers, A.B. Dalton, L.M. Evans, and H.J. Byrne, *Chem. Phys. Lett.* **345**, 361 (2001).
13. M.E. Kornienko, *Quant. Elektr.* **12**, 1595 (1985).
14. M.E. Kornienko, *Ukr. Fiz. Zh.* **47**, 435 (2002).
15. M.E. Kornienko and S.I. Mikhnytsky, *Ukr. Fiz. Zh.* **47**, 545 (2002).
16. M.E. Kornienko and S.I. Mikhnytsky, *Ukr. Fiz. Zh.* **47**, 726 (2002).
17. M.E. Kornienko, *Visn. Kyiv Univ. Ser. Fiz. Mat. Nauky* **3**, 489 (2006).

Received 22.10.09.

Translated from Ukrainian by H.G. Kalyuzhna

ТОНКА СТРУКТУРА СМУГ У КОЛИВАЛЬНИХ СПЕКТРАХ ФУЛЕРИТУ C_{60}

М.Є. Корнієнко, М.П. Куліш, С.А. Алексєєв, О.П. Дмитренко

Резюме

Досліджено тонку структуру низькочастотних коливальних смуг у спектрах комбінаційного розсіяння (КР), інфрачервоного поглинання і дифузного відбивання фулериту C_{60} . Вона пов'язана із компонентами давидівського та ізотопного розщеплення, які перекриваються, а також можливим зняттям виродження коливань внаслідок пониження симетрії. Показано, що для КР смуг $H_g(1)$, $A_g(1)$ та ІЧ-смуг $F_u(1,2)$ величини розщеплень при кімнатній температурі більші, ніж у низькотемпературній фазі. Підсилення міжмолекулярної взаємодії у випадку підвищених температур пояснюється нерівноважним коливальним збудженням середовища в результаті нелінійної взаємодії коливальних мод і зміною електронних станів.